Pharmaceutical Research, Vol. 25, No. 7, July 2008 (© 2008)
DOI: 10.1007/s11095-008-9573-8

Research Paper

The Asymmetry of the Unstirred Water Layer in Permeability Experiments

Timo Korjamo,[1,3] Aki T. Heikkinen,[1] Pekka Waltari,[2] and Jukka Mönkkönen[1]

Received January 19, 2008; accepted March 18, 2008; published online April 16, 2008

Purpose. To elucidate the apical and basolateral components of the total unstirred water layer in regular permeability experiment.
Methods. A novel stirring apparatus was constructed to remove the basolateral unstirred water layer. Caco-2 cells were used as the permeability barrier both in Transwell-type and side-by-side apparatuses. Permeability experiments were done with several ionisable compounds at various pH and stirring conditions. The permeabilities of the cell monolayer, the unstirred water layer and the polycarbonate filter were calculated either from experimental data or theoretically.
Results. The unstirred water layer was thicker in the Transwell apparatus than in the side-by-side chamber even in the presence of vigorous basolateral magnetic stirring. Calculations indicated that the apical unstirred water layer is thicker than the basolateral layer. Different cellular permeability coefficients were obtained from the two permeability apparatuses.
Conclusions. An orbital shaker does not produce symmetric hydrodynamics in both chambers of Transwell apparatus. The asymmetric unstirred water layer may complicate the exact analysis of polarized transport.

KEY WORDS: Caco-2; permeability experiment; unstirred water layer.

INTRODUCTION

Unstirred water layer (UWL) is the region of poorly stirred liquid next to the surface of a vessel. In this region, the diffusional movement of molecules exceeds the movement due convection and, thus, a concentration gradient is formed (6). UWL has been shown to control the apparent permeability of lipophilic molecules in *in vitro* permeability experiments (1,9). Therefore, the applied stirring rate is crucial if such molecules are to be studied.

A typical *in vitro* permeability experiment is conducted in a Transwell (TW) type of plate using an orbital shaking. This apparatus has asymmetric geometry with respect to apical and basolateral compartments. The apical compartment has a free air-to-liquid interface on top of the cell monolayer while the basolateral space is only 1 mm in depth and restricted by solid surfaces. Therefore, the UWL in the upper (apical) and lower (basolateral) compartments may be different. However, the total measurable UWL resistance is usually considered to be equally distributed on both sides of the monolayer (1,5). Whether the UWL is symmetric or asymmetric should not cause a major problem if the studied molecule is transported passively because, at least in theory, the total permeability resistance is the sum of the individual resistances and, therefore, only total thickness of the UWL is relevant. However, if the UWL resistances are not equal on both sides of the cell monolayer, apparent transport kinetics can be transport direction dependent. Such direction dependence has been described and explained by the differences in apical and basolateral membrane composition (21). Some reports suggest that UWL plays a role in the apparent kinetics of both influx (5) and efflux (12) transporter substrates. The present literature describes only total UWL resistances in Transwell apparatuses (1,9). In addition, some alternative apparatuses have been devised to study the UWL (8,10,23) but these do not reflect the UWL in commonly used Transwell apparatus. Thus far, there are no reports on attempts to dissect the UWL resistance into apical and basolateral components in the Transwell apparatus have been published.

To achieve this goal, a novel 12 place magnetic stirrer was constructed. The permeabilities of total and apical UWLs were determined without and with vigorous basolateral stirring. The UWL thickness was studied by both stirring (1,9,23) and pH (4,22) methods. In addition, the permeabilities were studied also in a side-by-side (SbS) apparatus to compare the hydrodynamics under these two different experimental settings.

[1] Department of Pharmaceutics, University of Kuopio, P.O. Box 1627, 70211 Kuopio, Finland.
[2] ABB Ltd., Helsinki, Finland.
[3] To whom correspondence should be addressed. (e-mail: Timo.Korjamo@uku.fi)

ABBREVIATIONS: AB, apical-to-basolateral; AB Stir, apical-to-basolateral with basolateral magnetic stirring; BA, basolateral-to-apical; BA Stir, basolateral-to-apical with basolateral magnetic stirring; SbS, side-by-side chamber; TW, TransWell apparatus; UWL, unstirred water layer.

MATERIALS AND METHODS

Chemicals

All model compounds were purchased either from Sigma (St. Louis, MO, USA) or from MP Biomedicals, (Irvine, CA, USA). Standard cell culture reagents were from BioWhittaker (Belgium). Fetal bovine serum was obtained from EuroClone (UK). High-performance liquid chromatography (HPLC) reagents were from Sigma (St. Louis, MO, USA) and J.T. Baker (The Netherlands).

Cell Culture

Caco-2 cells (ATCC HTB-37, Manassas, VA, USA) were cultured as previously described (11). Briefly, Caco-2 cells (passages 35–50) were maintained subconfluent in cell culture flasks and subcultured twice a week. In the permeability experiments, the cells were seeded onto either Transwell or Snapwell polycarbonate filters (Catalog number 3401, translucent, membrane diameter 12 mm, pore size 0.4 μm, membrane thickness 10 μm; Corning Life Sciences, Corning, NY, USA). The cells were grown for 21–24 days prior to the permeability experiments.

Permeability Experiments

The model compounds and their physicochemical properties are given in Table I. The compounds were selected to span a range of lipophilicities and, hence, permeabilities. The compounds are known traverse the cells primarily passively with the exception of verapamil which is a substrate for P-glycoprotein. The compounds were used in a mixture, each at 50 μM initial concentration. Drug concentrations in samples were analysed with HPLC-ultraviolet/fluorescence as described previously (18).

The bi-directional apparent permeability coefficients in TW apparatus were determined at four different pH values (5.8, 6.5, 7.0 and 7.4) and at four different verified stirring speeds (250, 320, 370 and 420 rpm) on an orbital shaker (Titramax 1000, Heidolph, Germany). The pH was always the same in the apical and basolateral chambers (no pH-gradient experiments were conducted). The transport medium was Hanks' balanced salt solution buffered with either 2-(*N*-morpholino)ethanesulfonic acid (5.8 and 6.5) or 4-(2-hydroxyethyl)-1-piperazineethanesulfonic acid (7.0 and 7.4). One set of experiments was conducted on regular Transwell plates (AB and BA). In the other set of experiments, the basolateral unstirred water layer was assumed to be removed by applying vigorous (1,600 rpm) magnetic stirring in the basolateral chamber using a custom-made magnetic stirrer (AB Stir and BA Stir). The magnetic stirrer was placed on the orbital shaker and the apical hydrodynamics were assumed to remain unaffected. Since the space below the filter is only 1 mm in depth, a special 3 mm thick mask was used to elevate the filter to create sufficient space to accommodate a small (2×2×7 mm) magnetic bar. The stirring did not damage the cell monolayer since mannitol permeability was essentially unchanged (1.99×10^{-6} *vs.* 2.25×10^{-6} cm/s).

Table I. Properties of the Model Compounds

		LogP[a]				
	pKa[a]	Neutral	Charged	MW	D^b	P_f^c
Metoprolol	9.56	1.95	−1.1	267.7	7.80	980
Propranolol	9.53	3.48	0.78	259.3	7.91	994
Verapamil	9.07	4.33	0.71	491.1	5.94	747
Ibuprofen	4.45	4.13	−0.15	260.0	7.90	993
Atenolol	9.54	0.22	N.R.	266.3	7.82	983
Antipyrine	1.44	0.56	N.R.	188.2	9.13	1,148

N.R. Not reported
[a] Data taken from (2).
[b] Aqueous diffusion coefficient at +37°C ($\times10^{-6}$ cm^2/s). Calculated using equation presented in (3) with temperature correction (4)
[c] Permeability across blank filter ($\times10^{-6}$ cm/s). Calculated according to Eq. 3

The experiments were designed to avoid mass balance problems. The initial apical volume was always 0.6 ml and the initial basolateral volumes were 1.6 and 2.6 ml in the absence and presence of the elevation mask, respectively. After the cells were washed twice and equilibrated for 20–30 min, all liquids were removed. The donor solution was applied either to the apical (AB and AB Stir) or to the basolateral (BA and BA Stir) compartment. After 5 min, fresh buffer was added to the receiver compartment and the magnetic stirring was started. Samples of 50 μl were withdrawn from both chambers and the experimental time was started. Thereafter, 50 μl samples from both chambers were taken at 5, 20 and 40 min. No replacements were made and, therefore, there were no sudden changes in concentrations. The apparent permeability coefficients were calculated using iterative equation that accounts of the changes in concentration gradient and back-flux (17)

$$C_{R,b} = \frac{M}{V_R + V_D} + \left(C_{R,a} - \frac{M}{V_R + V_D}\right) e^{-P_{app}\times A\frac{V_R+V_D}{V_R\times V_D}\Delta t} \quad (1)$$

where $C_{R,a}$ and $C_{R,b}$ are receiver concentrations at the beginning and at the end of time interval a to >b, M is the total amount of drug at the beginning of time interval, V_D and V_R are the donor and receiver volumes, A is the area of the filter, P_{app} is the apparent permeability coefficient and Δt is the length of the time interval. Data from two time intervals (5 to 20 and 20 to 40 min) were used for the non-linear least-squares fitting which was calculated with Microsoft Excel software. The experiments were conducted twice in triplicate.

To compare the hydrodynamics of orbitally shaken TW to a well stirred situation, the permeabilities were also measured in a SbS chamber (PermeGear, Inc., Bethlehem, PA, USA). A Snapwell insert (similar to Transwell inserts, catalog number 3407) was fitted between the chambers. The area of the hole between the chambers was 0.64 cm^2 and both chambers had magnetic stirring (500 rpm). The initial volumes were 3.8 ml (apical) and 3.3 ml (basolateral) and a sample of 100 μl was withdrawn from both chambers at 0, 10, 20, 30 and 60 min without buffer replacements.

Atenolol served as the integrity control. If its permeability was unexpectedly high in one well then all data from that particular replicate were discarded. All experiments were conducted twice with three parallel wells. Since the charge

state of antipyrine is virtually zero throughout the applied pH-range, it was used as a control of passive transcellular permeability under different pH conditions.

The total permeability was assumed to consist of UWL, cell monolayer and filter permeabilities

$$\frac{1}{P_{obs}} = \frac{1}{P_{uwl,A}} + \frac{1}{P_c} + \frac{1}{P_f} + \frac{1}{P_{uwl,B}} \quad (2)$$

where P_{obs} is the observed apparent permeability, $P_{uwl,A/B}$ is the permeability of the unstirred water layer on the apical/basolateral side, P_c is the permeability across the cell monolayer and P_f is the permeability across the polycarbonate filter. The term $1/P_{uwl,B}$ was assumed to be zero when basolateral magnetic stirring was applied.

The apparent permeability of the filter was calculated as previously proposed (9)

$$P_f = \frac{D\varepsilon}{h} \quad (3)$$

where D is the aqueous diffusion coefficient (Table I) calculated with the equation presented in (3) using temperature correction (4), ε is the porosity of the filter calculated according to the manufacturer's documentation (0.4 μm pore diameter, 1×10^8 pores per square centimeter yielding a nominal porosity of 0.126) and h is the thickness of the filter (10 μm). Since the permeability of the filter is independent of the ionization of the molecule and it was also assumed to be independent of stirring, P_f was subtracted from the observed permeabilities to obtain the corrected apparent permeabilities for curve fitting.

$$\frac{1}{P_{app}} = \frac{1}{P_{obs}} - \frac{1}{P_f} \quad (4)$$

Analysis of the Thickness of the Unstirred Water Layer

Two approaches were used to analyze the thickness of the unstirred water layer. The first is based on the change of the ionization state of acidic and basic molecules (4,22)

$$\frac{1}{P_{app}} = \frac{1}{P_{uwl}} + \frac{1}{P_c} = \frac{1}{P_{uwl}} + \frac{1}{f_u P_u + f_i P_i} = \frac{1}{P_{uwl}} + \frac{1}{f_u(P_u - P_i) + P_i} \quad (5)$$

where P_{app} is the apparent permeability corrected for filter permeability, P_{uwl} is the permeability of the unstirred water layer, P_c is the permeability across the cell monolayer, P_u and P_i are the permeabilities of the unionized and ionized species across the cell monolayer and f_u is the fraction of the unionized species. For fitting purposes, the equation was transformed into a logarithmic form

$$\log P_{app} = -\log(f_u(P_u - P_i) + P_i + P_{uwl}) + \log P_{uwl} + \log(f_u(P_u - P_i) + P_i) \quad (6)$$

The data from different pH values at a constant stirring rate were analyzed with Eq. 6. The fitting for metoprolol, propranolol and ibuprofen was constrained by setting the P_u and P_i values to be equal in all directions at all stirring rates. The reported P_{uwl} values are averages of AB and BA values. Because verapamil is a P-glycoprotein substrate, its AB and AB Stir data were treated separately from BA and BA Stir data.

The second approach is based on changing the stirring speed while keeping the monolayer permeability constant (pH is constant) (1,9). It is assumed that the P_{uwl} can be described as a function of the stirring rate

$$P_{uwl} = K\nu^{\alpha} \quad (7)$$

where K is a fitted constant relating stirring speed to permeability, ν is the stirring speed and α is an exponent proposed to reflect the type of hydrodynamics (1). Thus, the apparent permeabilities can be fitted into

$$\frac{1}{P_{app}} = \frac{1}{P_{uwl}} + \frac{1}{P_c} = \frac{1}{K\nu^{\alpha}} + \frac{1}{P_c} \quad (8)$$

The curve fitting was constrained so that each pair (same pH, same basolateral stirring, e.g. AB 6.5 and BA 6.5 or AB Stir 7.4 and BA Stir 7.4) was forced to have the same values of K, α and P_c. Each verapamil data set were, however, analyzed separately since its cellular permeability was assumed to be asymmetric.

All curve fittings were done using Prism 4.0 software (GraphPad Software Inc., San Diego, CA, USA).

When the total ($P_{uwl,total}$) and apical ($P_{uwl,a}$) UWL permeabilities were obtained, the $P_{uwl,b}$ was calculated by simple subtraction.

$$\frac{1}{P_{uwl,B}} = \frac{1}{P_{uwl,total}} - \frac{1}{P_{uwl,A}} \quad (9)$$

The apparent thickness of the unstirred water layer was finally calculated by

$$h_{uwl} = \frac{D}{P_{uwl}} \quad (10)$$

where D is the aqueous diffusion coefficient.

RESULTS

The observed permeabilities of model compounds are presented in Table II. Only a few filters were discarded because of elevated atenolol permeability (data not shown). The permeability of antipyrine was pH independent and, thus the change in pH did not change considerably passive permeability properties of the monolayer (data not shown). Generally, propranolol, verapamil and ibuprofen permeabilities were of similar magnitude while that of metoprolol was lower. The ionization state clearly affected the observed permeabilities. In TW at pH 5.8, the permeability of metoprolol appears to be rate limited purely by the cell monolayer since it is independent of stirring conditions. In addition, the observed permeability value was very close to the calculated P_{cell} value (Table V). However, a considerably higher permeability of metoprolol was observed in SbS. The stirring rate affected the observed permeability in all other

Table II. Observed Bidirectional Permeabilities of Model Compounds ($\times 10^{-6}$ cm/s). Mean±SD

		Transwell system[a]					Side-by-side	
	pH	rpm	P_{obs} AB	P_{obs} BA	P_{obs} AB Stir	P_{obs} BA Stir	rpm	P_{obs} AB
Metoprolol	5.8	250	14±2	17±2	14±2	16±2		
		320	14±2	18±1	12±2	14±1		
		370	15±1	21±1	13±2	15±2		
		420	16±2	19±2	12±2	15±3	500	41±1
	6.5	250	39±6	39±2	40±6	45±3		
		320	47±15	44±6	39±3	48±9		
		370	46±7	56±4	48±7	47±4		
		420	49±4	57±6	48±6	47±2	500	110±3
	7.0	250	48±6	59±6	71±6	70±5		
		320	73±3	75±8	75±8	88±8		
		370	92±7	88±5	84±5	97±7		
		420	99±10	103±4	95±11	117±16	500	150±9
	7.4	250	69±7	67±13	90±4	105±15		
		320	95±8	98±6	111±9	129±6		
		370	113±5	122±10	115±10	143±11		
		420	137±7	128±9	148±13	150±14	500	210±1
Propranolol	5.8	250	50±5	57±6	56±6	72±4		
		320	60±10	66±9	60±8	74±11		
		370	68±5	82±5	64±4	77±4		
		420	75±4	84±9	68±10	85±11	500	160±6
	6.5	250	73±14	73±7	103±15	118±6		
		320	110±23	97±15	104±12	136±27		
		370	108±15	120±7	150±18	135±11		
		420	125±8	130±12	159±18	154±11	500	250±5
	7.0	250	79±9	77±7	128±13	121±5		
		320	113±6	107±17	147±9	168±26		
		370	161±13	134±9	174±13	207±16		
		420	186±26	161±5	224±16	254±16	500	280±21
	7.4	250	75±10	72±11	127±14	137±27		
		320	112±12	108±8	158±16	198±10		
		370	167±30	151±12	216±35	254±22		
		420	221±13	161±11	277±19	296±22	500	310±1
Verapamil	5.8	250	35±5	53±5	34±6	66±2		
		320	45±9	63±10	43±6	69±16		
		370	55±8	73±7	42±1	73±4		
		420	60±8	79±10	46±8	76±10	500	140±6
	6.5	250	56±7	67±9	77±11	99±6		
		320	82±24	91±16	67±13	119±32		
		370	78±21	93±9	102±17	109±11		
		420	99±8	111±16	102±7	120±22	500	210±26
	7.0	250	49±9	59±6	81±13	85±9		
		320	93±6	90±21	95±17	140±18		
		370	112±7	125±19	102±19	169±32		
		420	143±16	134±10	144±21	188±11	500	230±25
	7.4	250	57±6	64±14	86±14	116±19		
		320	91±8	98±13	130±28	154±10		
		370	115±14	137±23	154±18	173±13		
		420	174±15	140±11	190±40	219±260	500	312±9
Ibuprofen	5.8	250	93±6	114±3	149±9	155±25		
		320	121±9	117±11	202±27	187±8		
		370	191±9	181±14	306±32	256±29		
		420	225±42	183±21	318±45	260±42	500	330±22
	6.5	250	88±24	110±14	173±18	167±21		
		320	133±9	140±19	167±15	184±15		
		370	166±40	205±16	255±19	254±24		
		420	161±26	203±29	271±71	209±13	500	280±5
	7.0	250	80±14	82±15	122±4	99±9		
		320	116±3	123±10	147±13	157±20		
		370	164±12	153±10	158±16	203±11		
		420	165±34	192±17	231±26	238±12	500	230±13
	7.4	250	74±9	81±14	112±11	122±16		

Table II. (continued)

pH	Transwell system[a]					Side-by-side	
	rpm	P_{obs} AB	P_{obs} BA	P_{obs} AB Stir	P_{obs} BA Stir	rpm	P_{obs} AB
	320	92±8	109±8	113±13	139±4		
	370	118±27	148±13	141±23	162±12		
	420	129±9	149±9	159±23	174±7	500	160±10

[a] The experiments were conducted in the apical-to-basolateral or basolateral-to-apical directions on an orbital shaker. The inclusion of the basolateral magnetic stirring is indicated (AB Stir and BA Stir).
AB apical-to-basolateral direction, BA basolateral-to-apical direction

instances. With the exception of basic compounds at pH 5.8, basolateral stirring could increase the permeability when compared to orbital shaking only. The experimental permeabilities in TW approached the permeabilities in SbS when orbital stirring was high and basolateral magnetic stirring was applied. The highest observed permeabilities were around 300×10^{-6} cm/s.

The data show that the *in vitro* metoprolol permeability can vary between 14 and 140 in the physiological pH range, depending on the applied stirring rate (Table II). This may partly explain the extensive interlaboratory variability in Caco-2 permeability results. Figure 1 shows the relative contribution of the cell monolayer, filter and UWL resistance to the total permeability at the low (metoprolol AB pH 5.8) and high (ibuprofen AB Stir pH 5.8) extremes of apparent permeabilities in the Transwell apparatus. Metoprolol is rate limited primarily by the cell monolayer while ibuprofen

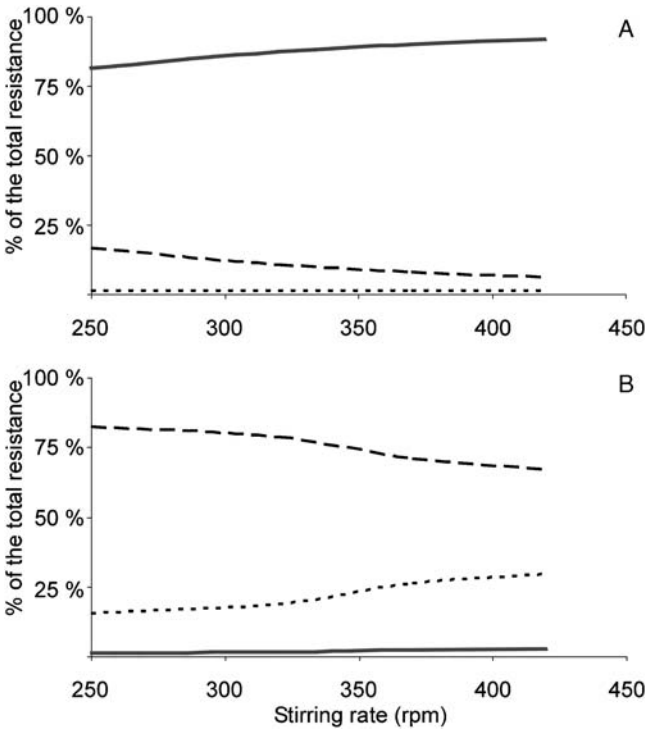

Fig. 1. The relative contribution of the cell monolayer (*solid line*), filter (*dotted line*) and UWL (*dashed line*) to the overall permeability resistance of metoprolol AB (**A**) and ibuprofen AB Stir (**B**) at pH 5.8 at different orbital stirring rates.

permeability is governed by aqueous diffusion through the UWL and the filter.

The experimental data (antipyrine, metoprolol, propranolol, verapamil and ibuprofen) did not fit properly into Eq. 8. The intercept ($1/P_{cell}$) was in most instances negative despite changing the stirring exponent, rendering the results physiologically meaningless (data not shown).

The P_{uwl} values and the corresponding apparent UWL thicknesses are presented in Table III. The apparent thickness of the total UWL ($h_{uwl,total}$) in TW ranged from 180 to 920 μm depending on the stirring rate and compound. The $h_{uwl,total}$ in TW was always larger than the corresponding value in SbS. $h_{uwl,A}$ in TW at the highest orbital stirring rate approached but generally did not reach $h_{uwl,total}$ in SbS. The $h_{uwl,total}$ values in TW for basic compounds were of similar magnitude. $h_{uwl,total}$ for acidic ibuprofen was somewhat lower. In contrast, $h_{uwl,A}$ of metoprolol in TW was larger than $h_{uwl,A}$ for the remainder of the compounds. Similarly, metoprolol seemed to display the thickest UWL in SbS. The calculated $h_{uwl,B}$ was smaller than $h_{uwl,A}$ at all stirring rates.

The experimentally determined P_{uwl} values were fitted to Eq. 7 (Table IV). The constant term K was very variable as the obtained values spanned several orders of magnitude. The stirring exponent α was mostly between 1.8 and 2.6, the only exception being the $P_{uwl,A}$ of metoprolol.

P_u and P_i were obtained from global fitting of the experimental data of a compound into Eq. 6 (Table V). The P_u and P_i for all basic compounds were considerably higher in SbS than in TW. In contrast, these values for ibuprofen were very similar in both apparatuses. The P_u initially increased as LogP increased but seemed to decline after a LogP value of 4. The permeability of the charged metoprolol species was in the range of paracellular permeability in TW but considerably higher in SbS. The more lipophilic compounds appeared to be able to traverse the cell membranes also in their charged forms. There was a moderate difference in verapamil permeability between the AB and BA directions. The calculated cellular permeability of metoprolol at pH 5.8 was similar to the observed permeabilities. In all other instances, the calculated P_{cell} values were clearly higher than the experimentally observed permeabilities. The ratio P_u/P_i varied between 1,000 and 18,000.

DISCUSSION

The unstirred water layer has an established effect in *in vitro* permeability assays (1,4,9). This work describes a novel

Table III. Apparent Permeabilities Across the Unstirred Water Layer and the Calculated UWL Thicknesses

	Transwell system							Side-by-side		
	rpm	$P_{uwl,total}$[a]	$h_{uwl,total}$[c]	$P_{uwl,A}$[a]	$h_{uwl,a}$[c]	$P_{uwl,B}$[b]	$h_{uwl,b}$[c]	rpm	$P_{uwl,total}$[a]	$h_{uwl,total}$[c]
Metoprolol	250	85±1	920±13	130±2	600±8	240	320			
	320	140±2	570±10	170±3	460±8	680	120			
	370	190±3	410±7	200±3	380±5	3,310	24			
	420	230±4	330±5	260±6	300±7	2,130	37	500	320±24	240±18
Propranolol	250	95±1	830±8	170±2	470±5	220	360			
	320	140±2	550±7	230±3	340±4	380	210			
	370	210±2	380±4	330±4	240±3	570	140			
	420	260±3	300±3	460±6	170±2	630	130	500	460±25	170±9
Verapamil	250	73±1	820±15	120±3	480±11	180	340			
	320	120±3	480±11	180±5	330±9	410	150			
	370	170±4	350±8	220±6	270±7	700	85			
	420	260±6	230±5	360±12	160±5	960	62	500	430±43	140±14
Ibuprofen	250	110±1	720±8	190±2	420±5	260	300			
	320	150±1	510±4	240±2	330±3	430	180			
	370	240±3	330±4	370±5	210±3	710	110			
	420	280±3	290±3	440±7	180±3	740	110	500	640±47	120±9

[a] Obtained from fitting the experimental data into Eq. 6. ($\times 10^{-6}$ cm/s). The reported number is the average from the corresponding AB and BA data. Mean±SE
[b] Calculated using Eq. 9 ($\times 10^{-6}$ cm/s).
[c] Calculated from the corresponding P_{uwl} value using Eq. 10 (micrometer).

approach to remove basolateral stirring problems in the Transwell system. The permeability of several drug molecules across Caco-2 cells was assessed in Transwell apparatus (in the presence and absence of basolateral unstirred water layer) and in a well stirred side-by-side chamber. This is the first attempt to dissect the total observed UWL in apical and basolateral components. This kind of knowledge is of major importance when asymmetric transport is modeled. The present data suggest that the total UWL resistance in TW is present to a greater extent at the apical side of the membrane.

The primary objective was to dissect the total UWL resistance in TW into apical and basolateral components. The space below the filter is only 1 mm thick and, thus, the movement of liquid is greatly restricted in the basolateral chamber. Therefore, it would seem to be logical to presume that the basolateral chamber would possess a thicker UWL than its apical counterpart. However, the calculated $h_{uwl,B}$ values are lower than $h_{uwl,A}$ (Table III), in other words the apical UWL appears to be the principal hydrodynamic barrier. The stirring exponents further support this claim (Table IV). The apical UWL appears to control the overall hydrodynamics since α values are similar in the absence and presence of basolateral stirring. It is, however, possible that the apical and basolateral UWLs are not completely independent. The UWL is not a sharp edged zone but rather a continuous gradient where the liquid velocity ranges nonlinearly from near zero next to surface to its maximum value in the bulk phase (6,19,20). Similarly, a curved concentration gradient from the surface concentration to the bulk concentration is formed. The removal of the basolateral UWL increases the net flux of molecules. This may increase the apical UWL resistance analogous to a change in UWL thickness as a function of ion mobility reported previously (20). Furthermore, permeability equations are based on the fundamental concept that the net movement of molecules proceeds only in one dimension. However, the water layer below the membrane is only 1 mm in depth and the samples are taken from the side of the filter. Therefore, it is likely that a radial concentration gradient is formed in the basolateral side of the membrane and the initial assumptions of permeability equations do not hold. In addition, our assumption of total absence of the basolateral unstirred water layer may be invalid since regular magnetic stirring forms a small stagnant area near the center of the filter (19). The thinnest observed UWLs in stirred membrane systems are around 25 μm (6). Therefore, the $P_{uwl,A}$ values may still contain a basolateral component.

The P_f is also a crucial parameter when the unstirred water layers are analyzed. In our approach (experiments with and without basolateral UWL), the P_f only affects the $P_{uwl,A}$ value. Therefore, if P_f is overestimated, $P_{uwl,A}$ will be underestimated and vice versa. It has been suggested that

Table IV. Parameters Describing the Unstirred Water Layer as a Function of Stirring Rate

	$P_{uwl,total}$[a]	$P_{uwl,A}$[a]
Metoprolol		
K	0.0017±0.0011	0.049±0.047
α	1.97±0.12	1.42±0.16
Propranolol		
K	0.001±0.0008	0.001±0.0016
α	2.07±0.14	2.15±0.27
Verapamil		
K	0.00002±0.00004	0.0002±0.001
α	2.674±0.29	2.36±0.49
Ibuprofen		
K	0.0035±0.006	0.0078±0.013
α	1.872±0.31	1.812±0.28

[a] Data from Table III was fitted into Eq. 7. Mean±SE

Table V. Apparent Permeabilities of Unionized and Ionized Species Across the Cell Monolayer

						P_{cell} (at pH)[b]			
			P_u[a]	P_i[a]	P_u/P_i	5.8	6.5	7.0	7.4
Transwell	Metoprolol		73,000±3,000	4±1	18,250	17	68	200	510
	Propranolol		320,000±27,000	55±5	5,820	93	330	970	2,390
	Verapamil	AB	65,000±9,400	37±6	1,760	72	210	590	1,400
		BA	89,000±16,000	86±10	1,030	130	320	840	1,950
	Ibuprofen		220,000±40,000	120±44	1,770	9,520	2,060	740	370
Side by side	Metoprolol		190,000±26,000	16±5	11,880	50	180	540	1,320
	Propranolol		1,200,000±400,000	120±70	10,000	340	1,240	3,650	8,950
	Verapamil	AB	270,000±160,000	170±86	1,590	310	890	2,450	5,820
		BA	N.D.	N.D.	N.D.	N.D.	N.D.	N.D.	N.D.
	Ibuprofen		180,000±48,000	110±59	1,620	7,800	1,700	620	310
Literature	Verapamil[c]	AB	8,440	11	750	16	24	82	190
	Verapamil + BSA[c]	AB	16,900	13	1,350	22	58	160	370
	Metoprolol[c]	AB	44,700	2.7	16,600	10	42	125	310
	Metoprolol[d]	AB	29,500±2,000	10±0.5	3,100	15	35	91	212
	Propranolol[c]	AB	33,600	29	1,200	35	60	130	280

N.D. not determined. Side-by-side experiments were conducted only in the AB direction.
[a] Cellular permeability of unionized/ionized species across the cell monolayer ($\times 10^{-6}$ cm/s)
Obtained from fitting the permeability data into Eq. 6. Mean±SE
[b] Total cellular permeability at a given pH calculated by $f_u \times P_u + f_i \times P_i$ ($\times 10^{-6}$ cm/s).
[c] P_u and P_i values taken from (4)
[d] P_{app} data from (15) was filter corrected and fitted into Eq. 6

the commonly used polycarbonate filters would have a true P_f value of about half of that calculated with Eq. 3 (23). The technical documentation of the filters also supports this possibility, since the manufacturer considers that as much as 60% difference may occur in the actual filter thickness compared to the nominal value of 10 μm. Therefore, $P_{uwl,A}$ maybe underestimated and, consequently, the true $h_{uwl,A}$ would be much thinner than Table III suggests. A previous work has described the possible effect of filter heterogeneity on the calculated UWL thickness in parallel artificial membrane permeability assays (16). The conclusion was that the variability in polycarbonate membrane porosity (0.05–0.2) leads to up to threefold difference in the calculated UWL height in such experiments. Therefore, the lack of exact knowledge on filter permeability can cause significant errors in the calculated UWL thicknesses. For comparison, all the calculations were performed also with 50% reduced P_f values (data not shown). Then $h_{uwl,B}$ was indeed thicker than $h_{uwl,A}$ in most cases. However, the $h_{uwl,total}$ in SbS was reduced to a value even less than 10 μm, which is not likely to be true. Unfortunately, it is impossible to determine the permeability across blank filter in TW since there is a considerable net flux of water across the filter, especially at high stirring rates. Therefore, the present calculations were conducted with the theoretical P_f. value.

The observed permeabilities in TW at different stirring conditions provide some indication for a threshold permeability beyond which the UWL becomes significant in TW (Table II). The data suggest that the limit would lie around 20×10^{-6} cm/s. However, the metoprolol data at pH 5.8 from SbS reveal that the TW suffers from poor hydrodynamics already at this level. In fact, all basic compounds show lower maximum permeability in TW than in SbS. In contrast, the highest observed ibuprofen permeabilities in TW were similar to those in SbS. This discrepancy between the two apparatuses may also originate from intracellular kinetics. The weakly basic molecules usually undergo lysosomal sequestration, called ion-trapping (7). In SbS, the volumes of donor and receiver chambers are considerably larger than in TW and, therefore, a small portion of the total drug amount is present in the kinetically slow compartment (lysosomes) in SbS than in TW. This may lead to a situation where steady state flux is not attained, despite an apparently constant mass balance. Acidic ibuprofen is not subjected to this intracellular sequestration and, hence, its behavior is similar in both apparatuses.

The literature often describes apparent thickness of the calculated UWL. Our results (Table III) are comparable to several published reports. Karlsson and Artursson (9) reported 128–1,544 μm UWL thickness at stirring rates 0–1,090 rpm and to Avdeef *et al.* (4) estimated the UWL thickness to be 381 μm for verapamil at 100 rpm, 303 μm for metoprolol at 450 rpm and 341 μm for propranolol at 450 rpm. Adson *et al.* (1) reported 220–930 μm for testosterone at 25–150 rpm. The stirring conditions in SbS are better than in TW but the apparent UWL thickness still does not achieve the values obtained in turbulent gas lift chambers (10,23) or the reported UWL thickness range of 30–100 μm in the intestine (13)

Equation 6 allows the estimation of the cellular permeability of neutral and charged form of acidic and basic compounds. Our results follow the general pattern that the permeability across cell monolayer increases as a function of lipophilicity but starts to decline with very lipophilic compounds (Tables I and V). The table also includes reported P_u and P_i data (4) and fitted values (Eq. 6) of metoprolol P_{app} data of Neuhoff *et al.* (4). The absolute values in this study are higher than those reported previously. In addition, the P_u/P_i-ratio was considerably higher than that described previously for rapidly transported alfentanil by Palm *et al.*

(17). The literature P_u and P_i data (Table V) were gathered under gradient-pH (basolateral receiver pH 7.4) conditions while we used iso-pH approach. It appears that our iso-pH conditions produced higher P_u and P_i values than the gradient experiments. All compared molecules were basic which makes the f_u larger in the receiver than in the donor compartment under physiological gradient-pH conditions and, thus, reduces the AB flux. This may also lead to reduction in the calculated cellular permeability values. The finding that basolateral sink conditions increase the P_u value of verapamil (4) and that our calculated P_u and P_i values for basic compounds were higher in SbS than in TW suggest that increase in apparent permeability results in higher fitted cellular permeability coefficients despite the actual membrane permeability probably remains unaltered. Naturally, also the applied fitting procedures (with possibly different weighting schemes) affect the obtained P_u and P_i values.

The present data also suggest that the P_{uwl} and, consequently, the h_{uwl} values are not equal for all compounds under identical stirring conditions (Table III). A similar observation has been made previously with Caco-2 data from various sources (4) and with a parallel artificial membrane permeability assay (16). The differences cannot be explained by aqueous diffusion coefficients since these are almost identical for metoprolol, propranolol and ibuprofen. The only common trend is that the higher the apparent permeability, the lower is the h_{uwl} observed both in TW and in SbS. This contrasts with the previous findings that an increase in ion mobility (permeability) leads to an increase in the UWL thickness (20). For stagnant point flow hydrodynamics, it may be possible to calculate the h_{uwl} for molecules based on one calibration molecule (20). However, in the case of less ideal mixing in *in vitro* permeability experiments, it is not likely that any general correlation can be calculated. Therefore, if accurate P_{uwl} and P_{cell} values are needed, the UWL resistance needs to be determined for each individual molecule.

The stirring exponent α is thought to depend on the type of hydrodynamics (1). Yet, only in a few ideal and symmetric cases can its value be calculated exactly (either 1/3 or 1/2) and the experimentally obtained values in reaction kinetic experiments are usually between 0.5 and 1 (14). The fitted exponent is therefore an abstract number without any true physiological meaning. It has been speculated that the relatively high fitted values in six-well TW plates (0.8) would reflect the asymmetric hydrodynamics (1). Avdeef *et al.* (4) analyzed the UWL resistance with three different molecules and obtained different exponents (0.89–1.22) that could describe the P_{uwl} as a function of the stirring rate. An early work found a linear (α=1) relationship between stirring rate and P_{uwl} (9). The present data set yielded considerably higher values for α (Table IV) which has been considered to reflect poorer stirring (1). In practice, this means that the UWL thickness is clearly dependent on the stirring rate. The discrepancy between the present data and published values may indeed originate from the hydrodynamics. Adson *et al.* (1) used a "break sandwich" procedure where the filter was frequently transferred into a new well which renews the basolateral sink. The more recent work by Avdeef *et al.* (4) was conducted with an orbital stirrer that has an orbit diameter of 3 mm while our stirrer has only 1.5 mm amplitude in its rotatory motion.. Naturally, this leads to considerable differences in the orbit speed at an equal angle speed. These differences are probably the main reasons accounting for different stirring exponents. It may also explain why the stirring method did not seem to work with the present data. Based on these observations, it can be concluded that UWL calculations derived from pH methodology are more robust than those based on the stirring rate methodology.

The present data emphasize the poor hydrodynamics in TW. A novel modification of traditional Transwell system has been introduced that greatly reduces the basolateral UWL thickness (12-place magnetic stirrer) and prolongs the time before the sink conditions are lost in a typical AB transport experiment (increase in basolateral chamber volume). Experiments with this apparatus indicate that the apical UWL appears to be at least an equally large resistance to permeability than the basolateral UWL despite the different geometries. However, the apical and basolateral UWLs are not independent of each other and, therefore, further studies on the possible asymmetry of the UWL in the Transwell apparatus and its effects on kinetics of actively transported compounds are warranted.

ACKNOWLEDGEMENTS

This study was financially supported by the Finnish Foundation for Technology and Innovation, The Finnish Cultural Foundation of Northern-Savo, Emil Aaltonen Foundation, The Association of Finnish Pharmacies and The Finnish Pharmaceutical Society. The skillful technical assistance from Mr. Markku Taskinen is gratefully acknowledged. The authors wish to thank Ewen MacDonald, Ph.D., for revising the language of the manuscript.

REFERENCES

1. A. Adson, P. S. Burton, T. J. Raub, C. L. Barsuhn, K. L. Audus, and N. F. Ho. Passive diffusion of weak organic electrolytes across Caco-2 cell monolayers: uncoupling the contributions of hydrodynamic, transcellular, and paracellular barriers. *J. Pharm. Sci* **84**:1197–1204 (1995).
2. A. Avdeef. *Absorption and Drug Development: Solubility, Permeability and Charge State*, Wiley, Hoboken, 2003.
3. A. Avdeef, P. E. Nielsen, and O. Tsinman. PAMPA—a drug absorption *in vitro* model; 11. Matching the *in vivo* unstirred water layer thickness by individual-well stirring in microtitre plates. *Eur. J. Pharm. Sci* **22**:365–374 (2004).
4. A. Avdeef, P. Artursson, S. Neuhoff, L. Lazorova, J. Grasjo, and S. Tavelin. Caco-2 permeability of weakly basic drugs predicted with the double-sink PAMPA pK(a)(flux) method. *Eur. J. Pharm. Sci* **24**:333–349 (2005).
5. A. Balakrishnan, N. Hussainzada, P. Gonzalez, M. Bermejo, P. W. Swaan, and J. E. Polli. Bias in estimation of transporter kinetic parameters from over-expression systems: interplay of transporter expression level and substrate affinity. *J. Pharmacol. Exp. Ther* **320**:133–44 (2007).
6. P. H. Barry and J. M. Diamond. Effects of unstirred layers on membrane phenomena. *Physiol. Rev* **64**:763–872 (1984).
7. M. Duvvuri, Y. Gong, D. Chatterji, and J. P. Krise. Weak base permeability characteristics influence the intracellular sequestration site in the multidrug-resistant human leukemic cell line HL-60. *J. Biol. Chem* **279**:32367–32372 (2004).
8. I. J. Hidalgo, K. M. Hillgren, G. M. Grass, and R. T. Borchardt. Characterization of the unstirred water layer in Caco-2 cell

monolayers using a novel diffusion apparatus. *Pharm. Res* **8**:222–227 (1991).
9. J. Karlsson and P. Artursson. A method for the determination of cellular permeability coefficients and aqueous boundary layer thickness in monolayers of intestinal epithelial (Caco-2) cells grown in permeable filter chambers. *Int. J. Pharm* **71**:55–64 (1991).
10. J. Karlsson and P. Artursson. A new diffusion chamber system for the determination of drug permeability coefficients across the human intestinal epithelium that are independent of the unstirred water layer. *Biochim. Biophys. Acta* **1111**:204–210 (1992).
11. T. Korjamo, P. Honkakoski, M. R. Toppinen, S. Niva, M. Reinisalo, J. J. Palmgren, and J. Mönkkönen. Absorption properties and P-glycoprotein activity of modified Caco-2 cell lines. *Eur. J. Pharm. Sci* **26**:266–279 (2005).
12. T. Korjamo, H. Kemilainen, A. T. Heikkinen, and J. Monkkonen. Decrease in intracellular concentration causes the shift in km value of efflux pump substrates. *Drug. Metab. Dispos.* **35**:1574–1579 (2007).
13. H. Lennernas. Human intestinal permeability. *J. Pharm. Sci* **87**:403–410 (1998).
14. V. G. Levich. *Physicochemical hydrodynamics*, Prentice Hall, Englewood Cliffs, 1962.
15. S. Neuhoff, A. L. Ungell, I. Zamora, and P. Artursson. pH-dependent bidirectional transport of weakly basic drugs across Caco-2 monolayers: implications for drug-drug interactions. *Pharm. Res* **20**:1141–1148 (2003).
16. P. E. Nielsen and A. Avdeef. PAMPA–a drug absorption *in vitro* model 8. Apparent filter porosity and the unstirred water layer. *Eur. J. Pharm. Sci* **22**:33–41 (2004).
17. K. Palm, K. Luthman, J. Ros, J. Grasjo, and P. Artursson. Effect of molecular charge on intestinal epithelial drug transport: pH-dependent transport of cationic drugs. *J. Pharmacol. Exp. Ther* **291**:435–443 (1999).
18. J. J. Palmgrén, J. Mönkkönen, E. Jukkola, S. Niva, and S. Auriola. Characterization of Caco-2 cell monolayer drug transport properties by cassette dosing using UV/fluorescence HPLC. *Eur. J. Pharm. Biopharm* **57**:319–328 (2004).
19. T. J. Pedley. Calculation of unstirred layer thickness in membrane transport experiments: a survey. *Q. Rev. Biophys* **16**:115–150 (1983).
20. P. Pohl, S. M. Saparov, and Y. N. Antonenko. The size of the unstirred layer as a function of the solute diffusion coefficient. *Biophys. J* **75**:1403–1409 (1998).
21. M. D. Troutman and D. R. Thakker. Efflux ratio cannot assess P-glycoprotein-mediated attenuation of absorptive transport: asymmetric effect of P-glycoprotein on absorptive and secretory transport across Caco-2 cell monolayers. *Pharm. Res* **20**:1200–1209 (2003).
22. D. Winne. Shift of pH-absorption curves. *J. Pharmacokinet. Biopharm* **5**:53–94 (1977).
23. H. Yu and P. J. Sinko. Influence of the microporous substratum and hydrodynamics on resistances to drug transport in cell culture systems: calculation of intrinsic transport parameters. *J. Pharm. Sci* **86**:1448–1457 (1997).